



Gliomas in children and adolescents: investigation of molecular alterations with a potential prognostic and therapeutic impact

Débora Cabral de Carvalho Corrêa^{1,2} · Francine Tesser-Gamba¹ · Indhira Dias Oliveira¹ · Nasjla Saba da Silva¹ · Andrea Maria Capellano¹ · Maria Teresa de Seixas Alves^{1,3} · Patrícia Alessandra Dastoli^{1,4} · Sergio Cavalheiro^{1,4} · Silvia Regina Caminada de Toledo^{1,2}

Received: 14 August 2021 / Accepted: 21 September 2021
© The Author(s), under exclusive licence to Springer-Verlag GmbH Germany, part of Springer Nature 2021

Abstract

Purpose Gliomas represent the most frequent central nervous system (CNS) tumors in children and adolescents. However, therapeutic strategies for these patients, based on tumor molecular profile, are still limited compared to the wide range of treatment options for the adult population. We investigated molecular alterations, with a potential prognostic marker and therapeutic target in gliomas of childhood and adolescence using the next-generation sequencing (NGS) strategy.

Methods We selected 95 samples with initial diagnosis of glioma from patients treated at Pediatric Oncology Institute-GRACC/ACC/UNIFESP. All samples were categorized according to the 2021 World Health Organization Classification of Tumors of the CNS, which included 39 low-grade gliomas (LGGs) and 56 high-grade gliomas (HGGs). Four HGG samples were classified as congenital glioblastoma (cGBM). NGS was performed to identify somatic genetic variants in tumor samples using the OncoPrint Childhood Cancer Research Assay[®] (OCCRA[®]) panel, from Thermo Fisher Scientific[®].

Results Genetic variants were identified in 76 of 95 (80%) tumors. In HGGs, the most common molecular alteration detected was *H3F3A* c.83A > T variant (H3.3 K27M) and co-occurring mutations in *ATRX*, *TP53*, *PDGFRA*, *MET*, and *MYC* genes were also frequently observed. One HGG sample was reclassified as supratentorial ependymoma *ZFTA*-fusion positive after NGS was performed. In LGGs, four *KIAA1549-BRAF* fusion transcripts were detected and this alteration was the most recurrent genetic event and favorable prognostic factor identified. Additionally, genetic variants in *ALK* and *NTRK* genes, which provide potential targets for therapy with Food and Drug Administration-approved drugs, were identified in two different cases of cGBM that were classified as infant-type hemispheric glioma, a newly recognized subgroup of pediatric HGG.

Conclusion Molecular profiling by the OCCRA[®] panel comprehensively addressed the most relevant genetic variants in gliomas of childhood and adolescence, as these tumors have specific patterns of molecular alterations, outcomes, and effectiveness to therapies.

Keywords Gliomas · Central nervous system tumor · Pediatric brain tumor · Congenital glioblastoma · Next-generation sequencing · Molecular profiling

Introduction

The fifth edition of the World Health Organization (WHO) Classification of Tumors of the Central Nervous System (CNS), published in 2021, introduces major changes involving the classification of gliomas, as this tumor is separated into pediatric-type and adult-type, given their well-established molecular and genetic differences. In this context,

gliomas occurring in children can be mainly categorized as low-grade and high-grade gliomas (Louis et al. 2021; Wen and Packer 2021).

Low-grade gliomas (LGGs) are a diverse spectrum of grade 1 and 2 tumors that represent the most common CNS neoplasms in children, accounting for approximately 30–40% of all primary pediatric brain tumors (Hargrave 2009). Pilocytic astrocytoma (PA) is the most frequent histological subtype of circumscribed astrocytic glioma in children and adolescents, and these patients frequently display an overall survival (OS) rate that can exceed 90% in 10 years. However, local recurrence occurs in 10–20%

✉ Silvia Regina Caminada de Toledo
silvatoledo@graacc.org.br

Extended author information available on the last page of the article

of cases and in patients where the primary lesion was not subjected to gross total resection, tumor progression rate is about 50–80% (Hargrave 2009; Jones et al. 2012). In contrast to adult LGGs, alterations in *IDH* gene are extremely rare in children, with the gain of 7q34 region of *BRAF* oncogene being the commonest mutation in childhood tumors (Drobysheva et al. 2017).

High-grade gliomas (HGGs) are malignant, diffuse, and infiltrating grade 3 and 4 tumors that represent 8–12% of all childhood CNS neoplasms. Pediatric patients with HGG show long-term OS rates lower than 10% and in most cases, these tumors are incurable. Childhood HGGs can be classified into subgroups based on their most recurrent genetic and epigenetic alterations (Braunstein et al. 2017; Fangusaro 2012). Somatic histone H3 alterations, such as K27M and G34R/V mutations, are specific molecular markers for pediatric HGGs. Recent studies have identified K27M mutation in *H3F3A* and *HIST1H3B* genes, responsible for encoding the H3.3 and H3.1 histone variants, respectively. Pediatric HGGs with *H3F3A* and *HIST1H3B* K27M alterations are midline tumors frequently observed in children that show a poor prognosis, while *H3F3A* G34R/V mutations occur in hemispheric tumors, are commonly identified in adolescents and young adults, and are associated with a slightly longer survival. Accordingly, these tumors comprise two main subgroups of pediatric HGG denoted as diffuse midline glioma H3 K27-altered and diffuse hemispheric glioma H3 G34-mutant (Ebrahimi et al. 2019; Sturm et al. 2014; Louis et al. 2021). Genome-wide methylation profiling of childhood HGG recently revealed six epigenetically distinct subgroups with alterations in *H3F3A* (H3.3 K27M and H3.3 G34R/V), *HIST1H3B* (H3.1 K27M), *IDH1/2* (*IDH*), and *BRAF* (*BRAF* V600E) genes (Pollack, Agnihotri, and Broniscer 2019).

Congenital brain tumors, defined by presentation prenatally or within the first months of life, represent approximately 2% of all pediatric CNS tumors, with congenital glioblastoma (cGBM) being among the rarest type (Solitare and Krigman 1964; Severino et al. 2010; Macy et al. 2012). To date, the most frequently genetic alterations identified in cGBM are *ALK* and *ROS1* gene fusions. Thus, recent studies have proposed that cGBM is genetically distinct from HGG that affects older children and adults, as these tumors harbor a unique molecular profile (Gilani et al. 2020; Macy et al. 2012). These findings suggest that cGBM may comprises a specific entity of infant-type hemispheric glioma, a novel tumor type recognized by the 2021 WHO Classification of Tumors of the CNS, characterized by newborns and infants that show fusions in *ALK*, *ROS1*, *NTRK*, or *MET* genes (Louis et al. 2021).

Therapeutic strategies for pediatric neoplasms, based on tumor molecular profile, are still limited compared to

the wide range of treatment options for the adult population (Ahmed et al. 2018; Lorentzian et al. 2018). The OncoPrint Childhood Cancer Research Assay® (OCCRA®) is the first next-generation sequencing (NGS) panel designed exclusively for the investigation of the main genetic events of childhood and adolescence neoplasms (Hiemenz et al. 2018). Considering the genomic and prognostic heterogeneity of pediatric and adolescent gliomas, as well as the unavailability of agents that target the most common molecular alterations present in these tumors, a specific NGS genetic panel can provide information for patients' stratification into risk groups and possible therapeutic targets (Pollack et al. 2019; Terashima and Ogiwara 2021).

Therefore, the present study aimed to investigate molecular alterations, with a potential prognostic marker and therapeutic target in gliomas of childhood and adolescence using the NGS strategy. We identified somatic genetic variants in tumor samples for a comprehensive molecular profiling of LGGs and HGGs using the OCCRA® panel.

Materials and methods

Tumor samples

All 95 fresh-frozen tumor samples used in this study were obtained from patients treated at Pediatric Oncology Institute-Grupo de Apoio ao Adolescente e à Criança com Câncer/Federal University of Sao Paulo (IOP-GRA ACC/UNIFESP), between 2000 and 2020, and belong to the Institute Biobank (National Commission of Ethics in Research—CONEP B-053). All 95 cases with initial diagnosis of glioma were identified via a retrospective database review. This study was approved by the Institutional Research Committee (Committee for Ethics in Research—Federal University of Sao Paulo no. 0915/2019) and written informed consent was obtained from all patients/guardians.

All primary tumors were classified according to the morphological characteristics of the tumor tissues analyzed by immunohistochemistry and based on the 2021 WHO Classification of Tumors of the CNS (Louis et al. 2021). All internal cases were jointly reevaluated by two or three pathologists of our Institution and inclusion criteria was histological diagnosis of WHO grade 1, 2, 3, and 4 glioma. Based on our molecular findings using NGS, one HGG sample was reclassified as supratentorial ependymoma (ST-EPN) *ZFTA*-fusion positive, and excluded from patients' clinical and survival analysis.

149 DNA and RNA isolation and quantification

150 Total DNA and RNA were extracted from frozen tumor sam-
 151 ples using FastPrep[®]-24 Tissue Ruptor (MP Biomedicals[®])
 152 and AllPrep DNA/RNA Mini Kit (QIAGEN[®]) according to
 153 the manufacturer's instructions. After extraction, samples
 154 were quantified in Nanodrop 2000[®] and in Qubit 3[®] fluorom-
 155 eter using Qubit RNA HS Assay Kit[®] and Qubit dsDNA HS
 156 Assay Kit[®] (Thermo Fisher Scientific[®]). The ratio between
 157 the 260 nm and 280 nm absorbances was used as quality
 158 control (QC) for the extractions. An A260/280 ratio between
 159 1.6–1.8 and 1.8–2.0 was adopted for DNA and RNA, respec-
 160 tively. Only samples with the expected QC standards were
 161 included in the study. After quantification, synthesis of
 162 complementary DNA (cDNA) was performed using 20 ng
 163 of total RNA according to the manufacturer's protocol of
 164 SuperScript Vilo IV[®] (Thermo Fisher Scientific[®]).

165 Library preparation

166 Sequencing libraries were prepared from 20 ng of DNA
 167 and 20 ng of cDNA from each tumor sample, following the
 168 manufacture's protocol for the OCCRA[®] (Thermo Fisher
 169 Scientific[®]). Amplicon libraries with barcodes specific to
 170 each sample were generated from DNA and cDNA, and
 171 automated clonal amplification was performed on the Ion
 172 Chef[™] System (Thermo Fisher Scientific[®]). Only the beads
 173 that were enriched with a unique template (monoclonal), that
 174 yielded reads of 25 bp or longer after a 3'15 bp-wide sliding-
 175 window quality trimming approach with q17 threshold, and
 176 which do not belong to the library internal controls, were
 177 considered for further analyses. After the preparation was
 178 completed, the libraries were loaded in the Ion 540[™] chip
 179 (Thermo Fisher Scientific[®]) and inserted on the Ion S5[™]
 180 System Sequencer (Thermo Fisher Scientific[®]).

181 Next-generation sequencing run

182 Sequencing was performed using 200-bp reads, and at the
 183 end of the sequencing run, the data generated by the large-
 184 scale sequencing was performed, and the quality for each
 185 reading was evaluated using Torrent Suite[™] software version
 186 5.2.1 (Thermo Fisher Scientific[®]). Only amplicon readings
 187 that showed a ratio between the forward and reverse prim-
 188 ers ≥ 0.6 and ≤ 1.4 were selected. The readings obtained were
 189 aligned to the hg19/GHCh37 human reference genome on
 190 the Torrent Suite[™] software and were considered readings
 191 with a minimum coverage of 2000 \times . The generated BAM
 192 files were analyzed using Integrative Genomics Viewer soft-
 193 ware (IGV Software, San Diego, CA, USA). The Variant
 194 Call Format files were obtained and the variants identified

were compared to the following databases: COSMIC, 195
 dbSNP, and ExAC. 196

Variant analysis using the OncoPrint Childhood Cancer Research Assay[®] panel

All tumor samples included in this study were subjected 199
 to targeted sequencing using the OCCRA[®] panel that com- 200
 prises a total of 255 tumor-associated genes (Table S1 201
 Supplementary Material). Sequencing analysis contains 202
 information about somatic variants, including multi-nucle- 203
 otide variants (MNVs), single-nucleotide variants (SNVs), 204
 insertions or deletions (InDels), copy number variations 205
 (CNVs), and gene fusions. Variants were classified accord- 206
 ing to class (SNV or InDel), functional effect (missense, 207
 nonsense, synonymous, frameshift, and nonframeshift), and 208
 clinical significance (pathogenic, likely pathogenic, uncer- 209
 tain significance, likely benign, and benign) according to 210
 FATHMM prediction scores (0–1), with score ≥ 0.7 classi- 211
 fied as pathogenic. For CNVs, samples with MAPD ≤ 0.35 212
 were considered in the study. Variant characteristics were 213
 evaluated using COSMIC, ClinVar, VARSOME, USCS 214
 Genome Browser, and Ensembl Genome Browser databases. 215

Data and statistical analysis

Data analysis was performed using IBM SPSS Statistics ver- 217
 sion 21.0 (Armonk, NY: IBM Corp), jamovi version 1.2 (The 218
 Jamovi Project, Sidney, AU), and GraphPad Prism version 219
 7.0 (GraphPad Software, San Diego, CA, USA) for Win- 220
 dows. OS curves were generated by applying Kaplan–Meier 221
 method with a 95% confidence interval (95% CI), and then 222
 compared by Log-rank test. Statistical significance was 223
 taken as $p < 0.05$ (5%). 224

Results

Patient and tumor characteristics

Clinical features of the patients analyzed in this study are 227
 summarized in Table 1 and molecular classification can be 228
 found in Table 2. The sex ratio was 1:1 (male: 51%; female: 229
 49%), and the median age at diagnosis was 5.8 years (range: 230
 0.3–16.6 years) and 7.5 years (range: 0–18.7 years) for LGG 231
 and HGG patients, respectively. 232

LGGs (grade 1/2) were comprised by 27 (29%) cases of 233
 PA, one (1%) case of ganglioglioma, a glioneuronal tumor, 234
 five (5%) cases of diffuse LGG MAPK pathway-wildtype, 235
 and five (5%) cases of diffuse LGG MAPK pathway-altered. 236
 One (1%) case included a pilomyxoid astrocytoma (PMA), 237
 a variant of PA that exhibits a more aggressive behavior. 238

Table 1 Clinical features of the patients analyzed in the study

Characteristic	Total (N=94)			
	Low-grade gliomas		High-grade gliomas	
	N=39		N=55	
	No.	%	No.	%
Age at diagnosis, years				
Median	5.8		7.5	
Range	0.3–16.6		0–18.7	
Mean	6.8		8.5	
Standard deviation	4.4		5.7	
Follow-up time, months				
Median	51.2		19.0	
5-year overall survival				
Rate	90.7%		24.6%	
10-year overall survival				
Rate	87.2%		12.3%	
Sex				
Female	23	59	23	42
Male	16	41	32	58
Tumor location				
Hemispheric	4	10	24	43
Diencephalic/Thalamic	1	3	13	24
Optic/Suprasellar	3	8	1	2
Ventricular/Intraventricular	2	5	3	5
Posterior Fossa	29	74	7	13
Spinal	0	0	7	13
Relapse				
Yes	6	15	11	20
No	33	85	44	80
Actual status				
Complete remission	22	56	10	18
In treatment	12	31	6	11
Dead	5	13	39	71
Treatment				
Chemotherapy	6	15	11	20
Radiotherapy	2	5	8	15
Chemotherapy + Radiotherapy	5	13	27	49
None	26	67	9	16

HGGs (grade 3/4) consisted of two (2%) cases of pleomorphic xanthoastrocytoma (PXA), one (1%) case of malignant ganglioglioma, 18 cases of H3 K27-altered gliomas, including 16 (17%) midline (diffuse midline glioma H3 K27-altered) and two (2%) hemispheric (diffuse glioma H3 K27-altered) tumors, one (1%) case of diffuse hemispheric glioma H3G34-mutant, 31 (33%) cases of diffuse HGG H3-wildtype and IDH-wildtype, and two (2%) cases of infant-type hemispheric glioma. One (1%) HGG sample was reclassified as ST-EPN *ZFTA*-fusion positive.

Table 2 Molecular classification of tumor samples analyzed in the study, according to the 2021 WHO Classification of Tumors of the CNS

Molecular classification	No.	%
Low-grade gliomas		
Pilocytic astrocytoma	27	29
Pilomyxoid astrocytoma	1	1
Diffuse low-grade glioma, MAPK pathway-wildtype	5	5
Diffuse low-grade glioma, MAPK pathway-altered	5	5
High-grade gliomas		
Pleomorphic xanthoastrocytoma	2	2
Diffuse midline glioma, H3 K27-altered	16	17
Diffuse glioma, H3 K27-altered	2	2
Diffuse hemispheric glioma, H3 G34-mutant	1	1
Diffuse high-grade glioma, H3-wildtype and IDH-wildtype	31	33
Infant-type hemispheric glioma	2	2
Glioneuronal and neuronal tumors		
Ganglioglioma	2	2
Reclassification		
Supratentorial ependymoma, <i>ZFTA</i> -fusion positive	1	1
	95	100

A total of 20 cases were infantile gliomas and four cases were classified as cGBM. Classification criteria for infant HGG was diagnosis under 5 years old (Clarke et al. 2020) and congenital cases consisted in those patients who presented clinical symptoms at birth, within the first weeks of life, or within the first 3 months of age. (Solitare and Krigman 1964). Among the four patients with cGBM analyzed, two patients had a postnatal diagnosis, with mean age at diagnosis of 1.3 months, and two patients were diagnosed during the prenatal. cGBM patients included four females and all tumors affected the cerebral hemispheres of the supratentorial compartment. Additionally, two cGBM cases were classified as infant-type hemispheric glioma, a newly recognized group of pediatric HGG (Louis et al. 2021).

Identification of genetic variants in glioma samples

A total of 95 samples with initial diagnosis of glioma were sequenced to investigate the presence of somatic genetic variants using the OCCRA[®] panel. Sequencing analyses showed that variants were detected in 76 of 95 (80%) tumors - 33 LGGs (43.4%) and 43 HGGs (56.6%). We observed 51 altered genes and 123 genetic variants, which included 60 SNVs (48.8%), 22 InDels (17.9%), 29 CNVs (23.6%), and 12 gene fusions (9.7%). *KIAA1549–BRAF* fusions were the most frequent events in LGGs (26/33 = 78.8%) and variants in *H3F3A* (17/43 = 39.5%), *TP53* (17/43 = 39.5%), and *ATRX* (9/43 = 20.9%) genes were responsible for the majority of all alterations identified in HGGs. The distribution

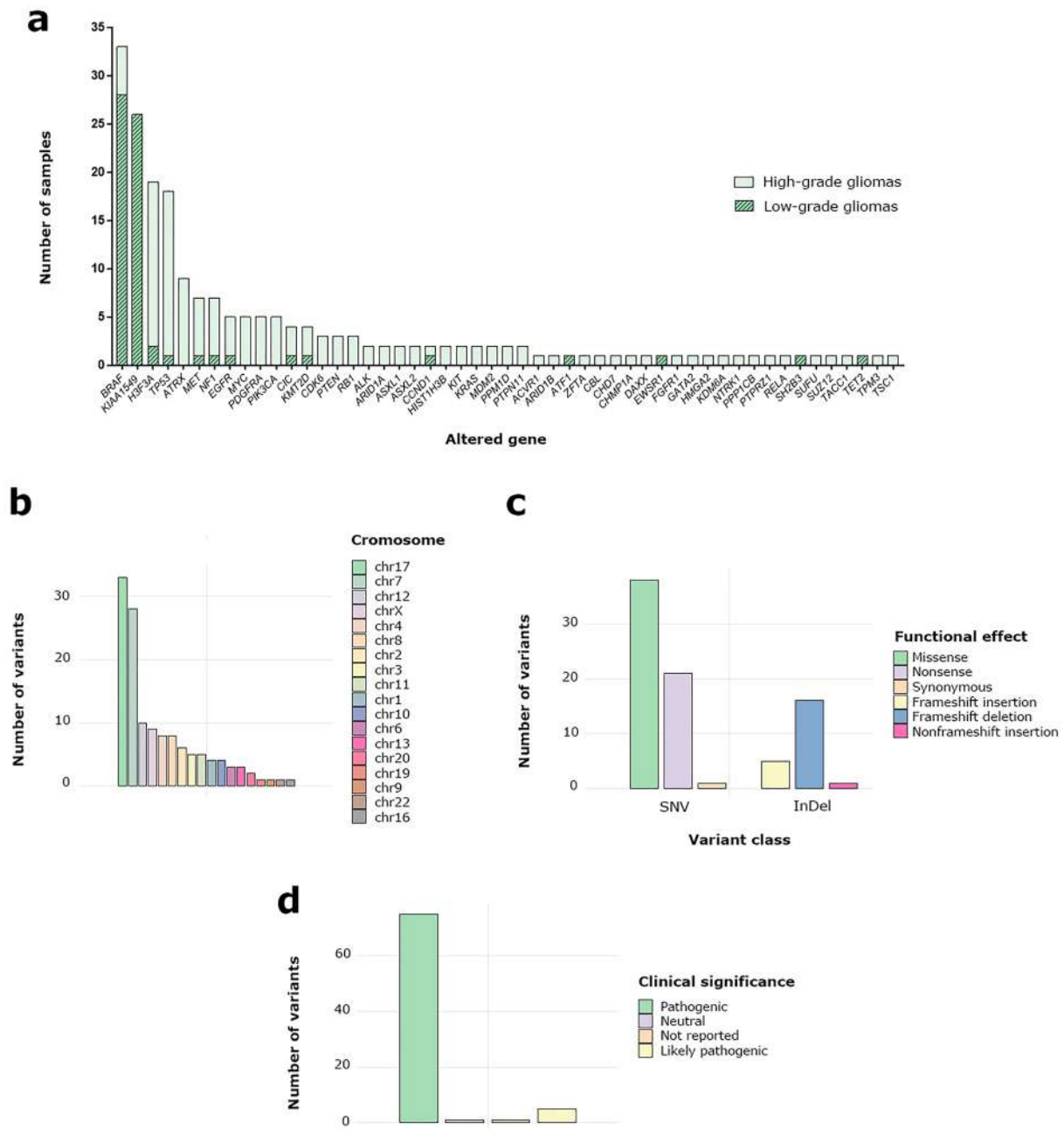


Fig. 1 Genetic alterations identified in tumor samples. **a** Frequency of mutations by gene in the 95 samples. **b** Number of variants located on each chromosome. **c** Number of variants according to class and functional effect. **d** Number of variants according to clinical significance

of altered genes in glioma samples is shown in Fig. 1a, and profile of genetic variants identified in tumor samples can be found in Table S2 (Supplementary Material).

Genetic variants analysis

Chromosome 17 had the highest number of variants (25%), followed by chromosome 7 (21.2%), as *TP53*, *KIAA1549*, and *BRAF* genes were the most frequently altered genes

detected in tumor samples and are located at 17p13.1 and 7q34, respectively. Variants with missense and nonsense effect were the most common, accounting for 46.3% and 25.6% of cases, respectively. InDels were also frequently identified, as frameshift deletion variants were responsible for 19.6% of cases, and frameshift insertions were observed in 6.1% of cases. Synonymous and nonframeshift variants were found in 1.2% of cases each (Fig. 1c). Of all variants analyzed, 91.5% were pathogenic,

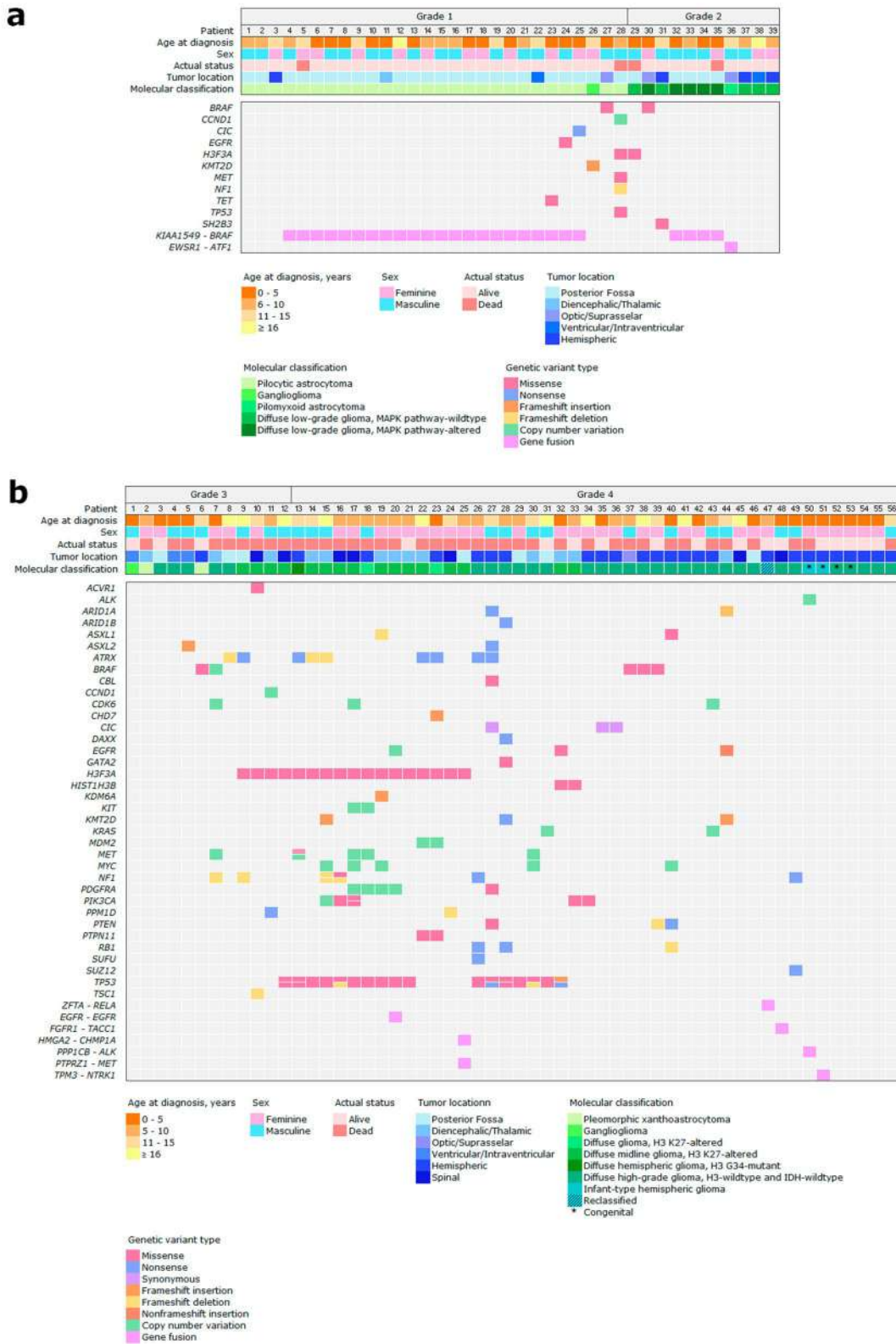


Fig. 2 Clinical and molecular profile of gliomas. **a** Genomic landscape of 39 LGG samples. **b** Genomic landscape of 56 HGG samples. Left pane indicates the altered gene across all the samples and each

vertical bar represents an individual case. The presence of more than one variant in the same gene is represented by multicolored boxes

Table 3 *KIAA1549–BRAF* fusion transcripts detected in LGG samples

Gene fusion	Gene 1			Gene 2			Total (N=26)	
	Name	Chr position	Exon	Name	Chr position	Exon	No.samples	%
<i>KIAA1549–BRAF</i>	<i>KIAA1549</i>	7:138552721	14	<i>BRAF</i>	7:140487384	9	8	30.8
	<i>KIAA1549</i>	7:138545885	15	<i>BRAF</i>	7:140487385	9	11	42.3
	<i>KIAA1549</i>	7:138545885	15	<i>BRAF</i>	7:140481493	11	6	23.1
	<i>KIAA1549</i>	7:138529062	17	<i>BRAF</i>	7:140482957	10	1	3.8

Chr chromosome

292 6.1% were likely pathogenic, 1.2% were neutral, and 1.2%
293 have not been reported yet (Fig. 1d).

294 Comprehensive molecular profiling of gliomas

295 The genomic landscape of LGG and HGG patients analyzed
296 in the present study using the OCCRA[®] panel can
297 be observed in Fig. 2a and b, respectively. A total of 26
298 *KIAA1549–BRAF* fusions were detected in LGGs, and
299 among them, 22 (84.7%) cases were identified in PA sam-
300 ples. Four *KIAA1549–BRAF* fusion transcripts were detected
301 and the most common was between exon 15 of *KIAA1549*
302 and exon 9 of *BRAF* (15;9), observed in 11 of 26 (42.3%)
303 cases. *KIAA1549–BRAF* fusions 14;9 and 15;11 were also
304 prevalent, observed in eight (30.8%) and six (23.1%) of 26
305 cases, respectively. Less common fusion transcript included
306 exon 17 of *KIAA1549* and exon 10 of *BRAF* (17;10), which
307 was identified in one case (3.8%) (Table 3). In addition, a
308 gene fusion between exon 7 of *EWSR1* and exon 5 of *ATF1*
309 (*EWSR1–ATF1*) was detected in one PMA sample in the
310 LGG subgroup.

311 In HGGs, c.83A > T (H3.3 K27M) and c.103G > A
312 (H3.3 G34R) variants of *H3F3A* gene were identified in
313 16 cases and one case, respectively. *BRAF* c.1799 T > A
314 variant (*BRAF* V600E) was observed in four cases, includ-
315 ing one PXA. No alterations in *IDH1* or *IDH2* genes were
316 detected by the panel. Interestingly, co-occurring altera-
317 tions were observed in HGG patients harboring variants in
318 *H3F3A* gene—58.8% (10/17) of cases had variants in *TP53*,
319 35.3% (6/17) of cases showed *ATRX* loss-of-function muta-
320 tions, 23.5% (4/17) of cases had *PDGFRA*-amplification,
321 and 35.2% (6/17) of cases showed *MET* or *MYC* amplifica-
322 tions. Moreover, three tumors had concomitantly variants
323 in *H3F3A*, *TP53*, and *ATRX* genes (Fig. 3a). A gene fusion
324 between exon 3 of *ZFTA* and exon 2 of *RELA* (*ZFTA–RELA*)
325 was detected in one HGG case that was reclassified as ST-
326 EPN *ZFTA*-fusion positive.

327 Of all four cGBM patients analyzed, two cases exhib-
328 ited tumors with genetic variants. One patient showed an
329 increase of 11.2 copies of *ALK* and a gene fusion between
330 exon 5 of *PPP1CB* and exon 20 of *ALK* (*PPP1CB–ALK*),
331 and one patient had a *NTRK* gene fusion, which consisted

in exon 7 of *TPM3* and exon 10 of *NTRK1* (*TPM3–NTRK1*)
(Table 4). Both tumors were classified as infant-type hemi-
spheric glioma.

Subgroup of HGG in children and adolescents with HGG subgroup with histone H3.3 mutations

H3F3A c.83A > T variant was responsible for the major-
ity of all genetic alterations detected in HGGs. Of all 16
H3.3 K27-altered gliomas analyzed in the present study,
14 affected midline regions of the CNS, which included
seven (43.8%) thalamic tumors, five (31.2%) spinal, and
two (12.5%) from the cerebellum/brainstem, whereas two
(12.5%) cases samples affected the cerebral hemisphere of
the supratentorial region. The only H3.3 G34 mutant tumor
identified was hemispheric (Fig. 3b).

HGG patients with H3.3 K27M mutation had a median
OS of 9.1 months (95% CI 4.0–14.3), and OS curves anal-
ysis showed a statistical difference between H3.3 K27-
altered ($n = 16$) and H3.3 K27-wildtype ($n = 13$) subgroups
($\chi^2 = 11.99$, $p = 0.0005$). Patients with H3.3 K27M mutation
had a worse 5-year OS (rate: 6.3%) in comparison to the
wildtype subgroup (rate: 61.5%) (Fig. 3c).

High frequency of DNA copy number variations in HGGs

Of all 29 CNVs detected by the panel, 28 (96.5%) were iden-
tified in HGGs. Increase in the copy number of 12 genes was
observed, with *MET* (5/28 = 17.8%), *MYC* (5/28 = 17.8%)
and *PDGFRA* (4/28 = 14.3%) genes being responsible for
the majority of cases. The median DNA copy number was
6.9 copies (range: 1.2–270 copies; standard deviation: 50.1)
and the distribution of all CNVs detected in HGG samples is
summarized in Table S3 (Supplementary Material).

Survival comparisons between tumor subgroups

LGG and HGG patients included in the study were observed
for a median of 51.2 months and 19 months, respectively,
from date of diagnosis to last contact or death. For LGG
patients, the median OS was 187.2 months (95% CI

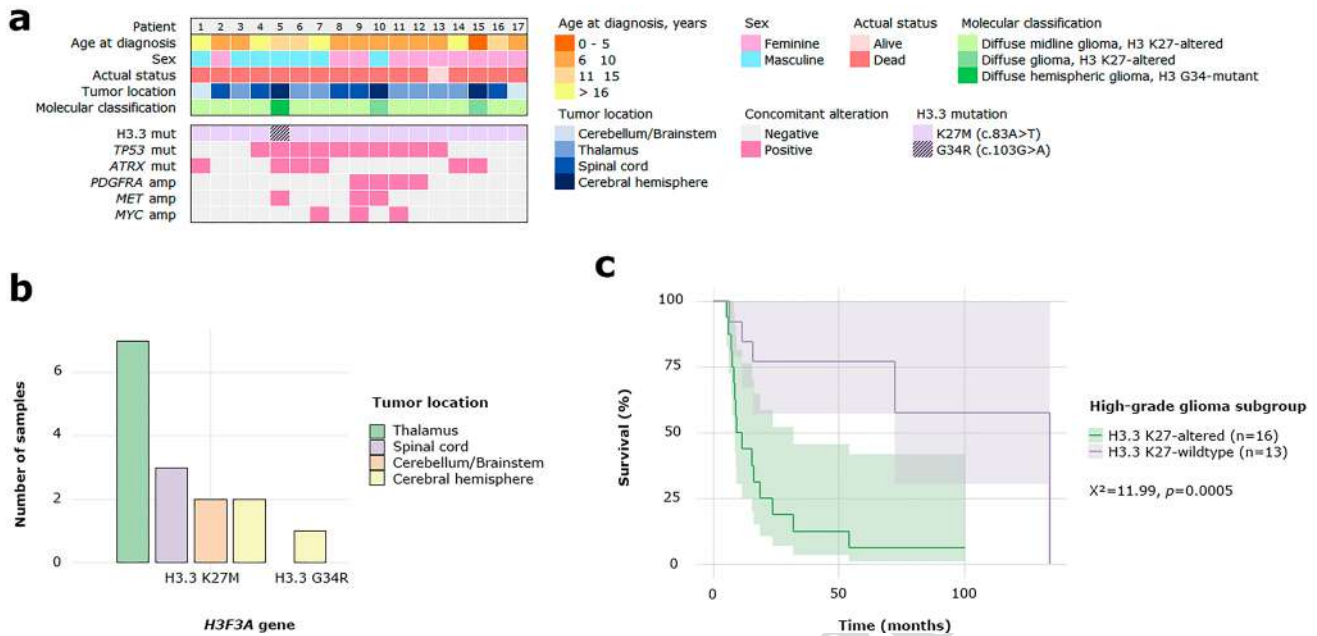


Fig. 3 Subgroup of HGG in children and adolescents with histone H3.3 alterations **a** Clinical and molecular profile of HGG patients with H3.3 K27M or G34R mutation (H3.3 K27M or H3.3 G34R) and concomitant variants involving *TP53*, *ATRX*, *PDGFRA*, *MET*, and *MYC* genes. **b** Number of samples with H3.3 K27M or G34R

mutation, according to tumor location. **c** Patients with H3.3 K27M-altered tumors showed a worse 5-year overall survival when compared to the wildtype subgroup ($\chi^2=11.99, p=0.0005$). *mut* mutation, *amp* amplification

368 182.5–191.8) and the 5-year and 10-year OS rates were
 369 90.7% and 87.2%, respectively. For HGG patients, the
 370 median OS was 23.6 months (95% CI 10.3–36.8) and
 371 the 5-year and 10-year OS rates were 24.6% and 12.3%,
 372 respectively.

373 OS curves showed a statistical difference between tumor
 374 subgroups ($\chi^2=34.59, p<0.0001$) (Fig. 4a), as HGG
 375 patients revealed a worse 10-year OS when compared to
 376 LGG patients. Also, infant patients with HGG (diagno-
 377 sis <5 years old; $n=20$) showed a better 10-year OS
 378 (rate: 45.7%) when compared to older patients with HGG
 379 (diagnosis >5 years old; $n=35$) (rate: 14.9%; $\chi^2=4.57$,
 380 $p=0.0324$) (Fig. 4b).

381 Discussion

382 Recent advancements in the molecular understanding
 383 of pediatric gliomas revealed that each tumor subgroup
 384 can harbor specific genetic alterations. However, the devel-
 385 opment of new targeted treatments for children and adoles-
 386 cents with glioma remains a major challenge (Terashima and
 387 Ogiwara 2021; Blattner-Johnson et al. 2021). Considering
 388 that gliomas in children differ on a clinical and molecu-
 389 lar basis from gliomas that occur in adults, we aimed to
 390 investigate the presence of somatic genetic variants, with

a potential prognostic and therapeutic impact in LGGs and
 HGGs of childhood and adolescence, for a comprehensive
 tumor profiling.

Mutations in *BRAF* gene represent the most frequently
 known and well-established genetic alterations in pediatric
 LGGs. *KIAA1549–BRAF* fusion is detected in 50–85% of
 PA, leading to deregulation of the *MAPK* signaling pathway
 (Jones et al. 2008; Kaul et al. 2012). Currently, there are nine
 known *KIAA1549–BRAF* fusion junctions, with the majority
 involving fusions between *KIAA1549* exon 16 and *BRAF*
 exon 9 (16;9) (68%), *KIAA1549* exon 16 and *BRAF* exon
 11 (16;11) (10%), and *KIAA1549* exon 15 and *BRAF* exon 9
 (15;9) (9%) (Srinivasa et al. 2020).

In the present study, *KIAA1549–BRAF* 15;9 was the most
 frequent fusion transcript detected in LGGs, accounting for
 42.3% of cases, a higher rate than the described in the lit-
 erature for this fusion variant. The second fusion transcript
 most detected, *KIAA1549–BRAF* 14;9 (30.8%), has not been
 reported in PA yet. Unexpectedly, 16;9 fusion transcript,
 commonly known as the most recurrent, was not identified
 in our tumor samples. Our clinical and molecular analysis
 revealed that *KIAA1549–BRAF* fusion was the most signifi-
 cant favorable prognostic factor in LGGs, since patients with
 this fusion had a 5-year OS rate of 100% and 95.7% of these
 patients showed no other additional alterations detected by
 the panel. It has been suggested that *KIAA1549–BRAF* may

Table 4 Clinical and molecular characteristics of four patients diagnosed with cGBM

Patient	Gender	Age at diagnosis	Tumor location	CNS region	Treatment	Status	Relapse	Overall survival	Variant class	Gene
1	Female	3 days	Hemispheric	Parietal	None	Dead	No	2.1 days	CNV	ALK
2	Female	2.5 months	Hemispheric	Occipital	Chemotherapy and radiotherapy	Alive	No	7.1 years	Gene fusion	PPP1CB-ALK
3	Female	Prenatal (31 weeks of gestation)	Hemispheric	Supratentorial	Chemotherapy	Alive	No	4.8 years	Gene fusion	TPM3-NTRK1
4	Female	Prenatal (unavailable data)	Hemispheric	Temporal	Chemotherapy	Alive	No	2.6 years	Negative	N/A

CNS central nervous system, SNV single-nucleotide variant, CNV copy number variation, N/A not applicable

lead to a less aggressive phenotype due to the process of oncogene-induced cell senescence. However, Federal Drug Administration (FDA)-approved therapies specific to this fusion are still lacking and current treatment options for LGGs involve targeting other alterations that dysregulate the *MAPK* pathway (Srinivasa et al. 2020). Consequently, identification of *KIAA1549–BRAF* fusions is essential in the context of clinical trials and treatment management for these patients.

In addition to *KIAA1549–BRAF*, *EWSR1–ATF1* fusion was also identified in one LGG case. Gene fusions involving *EWSR1* gene and members of the CREB family, such as *ATF1* gene, have been reported in a diverse group of tumors. Kao et al. (2017) investigated a cohort of children and young adults, aged 12–23 years old, with myxoid mesenchymal tumors positive for fusions between *EWSR1* and members of the CREB family, including *EWSR1–ATF1* fusion. These data suggest a new brain tumor type entitled intracranial myxoid mesenchymal tumors with *EWSR1* and CREB family gene fusions (*EWSR1–CREB*), and approximately 15 cases have been reported in the literature so far (Kao et al. 2017; De Los et al. 2021; Ballester et al. 2020; Liu et al. 2020). In our study, *EWSR1–ATF1* gene fusion was detected in a PMA sample that affected the optic region from a patient diagnosed with 12 years old. However, this tumor entity has not yet been recognized by the 2021 WHO Classification of Tumors of the CNS.

Recently, it has been proposed six epigenetically different subgroups of childhood HGGs that display alterations in *H3F3A*, *HIST1H3B*, *IDH1/2*, and *BRAF* genes (Pollack et al. 2019). H3.3 K27M mutation occurs in 70–80% of childhood HGGs, while H3.1 K27M variant is less frequent (Sturm et al. 2012; Venneti et al. 2013). *IDH* subgroup represents nearly 5% of all pediatric HGGs and tumors with *BRAF* V600E alteration are histologically similar to PXA, accounting for 5–10% of cases. Studies have reported that H3.3 K27M subgroup has a poor long-term survival, while *IDH* and *BRAF* subgroups show a comparatively favorable clinical outcome (Pollack et al. 2019). In our HGG samples, alterations in *H3F3A* gene were the most common events observed, *BRAF* V600E variant was identified in one PXA sample, and no alterations in *IDH1/2* were detected by the panel. Our findings show the presence of recurring molecular alterations, highlighting the genetic and prognostic diversity among these tumors, which consequently may further refine the classification of HGGs in children and adolescents (Pollack et al. 2019).

Genomic profiling analysis of pediatric and adolescent HGGs has shown that K27M and G34R alterations are mutually exclusive and intrinsically associated with the anatomic tumor location, with H3.3 K27M subgroup displaying predilection for the midline brain location, especially for the thalamic region, while H3.3 G34R subgroup

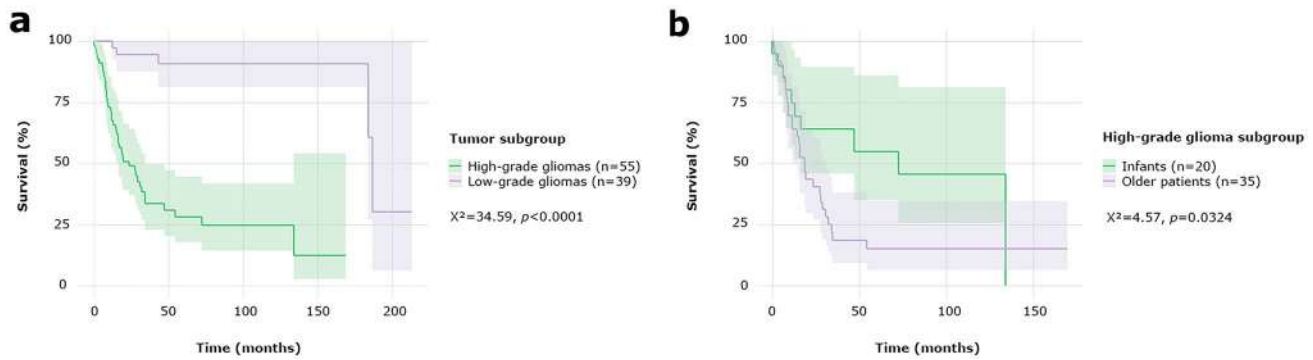


Fig. 4 Overall survival curves comparisons. **a** HGG patients showed a worse 10-year overall survival when compared to LGG patients ($\chi^2=34.59$, $p<0.0001$). **b** HGG patients diagnosed under 5 years old

(infant) had a better 10-year overall survival when compared to older patients with HGG ($\chi^2=4.57$, $p=0.0324$)

470 predominantly affects the cerebral hemisphere (Oliveira
471 et al. 2021; Schwartzentruber et al. 2012). Similarly, among
472 the HGG samples with H3.3 K27M mutation analyzed in
473 our study, 87.5% were midline and the only tumor harbor-
474 ing H3.3 G34R variant was hemispheric. Whereas G34R
475 mutation is highly expressed in the neocortex during the
476 early stages of embryonic development, K27M mutation is
477 associated with the intermediate and late stages of devel-
478 opment, mostly of the thalamic region. These evidences
479 indicate that HGGs harboring H3.3 K27M or H3.3 G34R
480 alterations have specific patterns of gene expression during
481 brain development that correlate with the subsequent tumor
482 location. Consequently, K27M and G34R mutations define
483 two clinically and biologically distinct subgroups of child-
484 hood HGGs (Sturm et al. 2012; Ebrahimi et al. 2019).

485 In our analysis, *H3F3A* variants simultaneously overlapped
486 with other specific alterations within the same tumor,
487 including *TP53* (58.8%) and *ATRX* (35.3%) loss-of-func-
488 tion mutations, and amplifications of *MET* (17.6%), *MYC*
489 (17.6%), and *PDGFRA* (23.5%) genes. Approximately 60%
490 of all H3.3 K27M mutations are associated with alterations
491 in *TP53* and 30% in *ATRX* (Deng et al. 2018; Huang et al.
492 2017; Yuen and Knoepfler 2013). Additionally, it has been
493 shown that tumors harboring H3.3 K27M mutation contain
494 higher numbers of CNVs, with *MYC* and *PDGFRA*
495 gene amplifications being the most commonly observed
496 (Schwartzentruber et al. 2012; Yuen and Knoepfler et al.
497 2013; Korshunov et al. 2015). A clinically significant find-
498 ing in our study was the fact that HGG patients with H3.3
499 K27-altered tumors had a worse 5-year OS in comparison
500 to the wildtype subgroup supporting the evidence that H3.3
501 K27M mutation is an adverse prognostic factor in pediatric
502 HGGs and these patients may benefit from therapies that
503 target chromatin remodeling agents or post-transcriptional
504 histone modifications.

505 To date, approximately 120 cGBM cases have been
506 reported and due to its infrequent occurrence, few studies

507 have focused on the molecular and genetic features of this
508 disease (Macy et al. 2012; Espiritu et al. 2020). In the pre-
509 sent study, an increase in the number of copies of *ALK* gene
510 and a *PPP1CB-ALK* fusion were identified in one cGBM
511 patient. Interestingly, Zhong et al. (2021) recently reported
512 a case of a female patient with cGBM that also died due to
513 disease progression two days after birth and showed genetic
514 alterations similar to those observed in our patient. They
515 detected an *ALK* amplification and a *PPP1CB-ALK* fusion,
516 which resulted of a local chromothripsis and consisted
517 of exon 1–5 of *PPP1CB* and exon 20–29 of *ALK* (Zhong
518 et al. 2021). Although several studies have shown that *ALK*
519 fusion proteins are present in a diverse group of neoplasms,
520 *PPP1CB-ALK* fusions have been reported in few cases in
521 the literature, mainly with respect to pediatric patients with
522 HGG. (Zhong et al. 2021; Aghajan et al. 2016; Guerreiro
523 Stucklin et al. 2019; Ng et al. 2019). Currently, efforts are
524 underway to develop small molecule tyrosine kinase inhibi-
525 tors (TKIs) that penetrate the blood–brain barrier, since ther-
526 apies targeting alterations in *ALK* gene have demonstrated
527 to improve overall outcomes in patients whose CNS tumors
528 arise from these genetic alterations (Holla et al. 2017; Wong
529 2017). *PPP1CB-ALK* fusions are one of the most com-
530 mon receptor tyrosine kinase fusions in infantile gliomas
531 and recent findings have demonstrated that tumor cells and
532 xenograph tumors positive for these fusions are sensitive to
533 *ALK*-inhibitors (Zhong et al. 2021; Guerreiro Stucklin et al.
534 2019; Amend et al. 2020). In this context, *PPP1CB-ALK*
535 fusion and *ALK* amplification may represent a set of poten-
536 tial biomarkers for cGBM.

537 *TPM3-NTRK1* fusion, which has already been shown
538 to act as an oncogenic driver in HGG (Hsiao et al. 2019),
539 was identified in one cGBM case in our study. Gliomas
540 can harbor *NTRK* fusions with frequencies of 5–25% and
541 *NTRK* fusions have been reported in up to 40% of non-
542 brainstem HGGs (NBS-HGGs) in patients under 3 year
543 sold (Amatu et al. 2016; Gambella et al. 2020; Clarke et al.

2020; Wu et al. 2014). Our cGBM patient, whose tumor was located hemispheric and is *TPM3-NTRK1* fusion-positive, was diagnosed with 2.5 months and showed no other significant additional alterations. These results seem to corroborate previous findings that have detected *TPM3-NTRK1* fusions in a particular subset of infant patients with NBS-HGGs (Clarke et al. 2020; Wu et al. 2014). *NTRK* fusion is a pharmacologically targetable genetic alteration and identification of fusion genes responsible for altering the activity of *NTRK* kinase domains has allowed the emergence of specific TKIs for these proteins (Lange and Lo 2018). Thus, multiple TKIs with activity against the tyrosine kinase family are available nowadays or being investigated in clinical trials. The first-generation TKIs, larotrectinib (Vitrakvi®) and entrectinib (Rozlytrek®), represent the two compounds that are furthest in clinical development so far, and were the first FDA-approved TKIs for adult and pediatric solid tumors with *NTRK* fusions (Rolfo 2020; Jiang et al. 2021).

The WHO Classification of Tumors of the CNS, published in 2021, has recognized a novel subgroup of HGG that occurs in newborns and infants with fusions in *ALK*, *ROS1*, *NTRK*, or *MET* genes, denoted as infant-type hemispheric glioma (Louis et al. 2021). None of our cGBM cases showed variants in *H3F3A*, *TP53*, and *ATRX* genes, alterations that are frequently seen in older children and adolescents with HGG. Instead, we identified variants in *ALK* and *NTRK* genes, suggesting that cGBM may comprise a specific entity of infant-type hemispheric glioma. Additionally, our survival analysis showed that infant patients with HGG have a more favorable prognosis with improved survival when compared to HGG in older children, which is in concordance with previous reports (Clarke et al. 2020; Gilani et al. 2020). These data indicate that histopathological grading may not truthfully reflect the clinical and biological aspects of these tumors, which highlights the need for an individualized diagnostic and therapeutic care. In such a young group of patients, chemotherapy and radiotherapy are limited approaches due to their significant long-term toxicity and in most cases, surgery and gross total resection represent the main treatment options. Hence, our findings emphasize the demand for age-specific diagnosis and treatment strategies, as identification of molecular alterations may provide potential therapeutic targets for these patients (Guerreiro Stucklin et al. 2019; Espiritu et al. 2020).

In conclusion, molecular profiling by the OCCRA® panel comprehensively addressed the most relevant alterations in gliomas of childhood and adolescence. *KIAA1549-BRAF* fusion was the most significant favorable prognostic factor in LGGs and *H3F3A* c.83A>T variant, commonly detected in HGGs, was associated with a worse OS in these patients. Alterations in *ALK* and *NTRK* genes were identified in two single cases of cGBM, which may provide potential targets for therapy with FDA-approved

drugs. Therefore, we were able to detect recurrent somatic mutations in LGGs and HGGs in children and adolescents, as these tumors have specific patterns of molecular alterations, outcomes, and effectiveness to therapies.

Supplementary Information The online version contains supplementary material available at <https://doi.org/10.1007/s00432-021-03813-1>.

Acknowledgements This study was conducted as a part of the “Investigation of genetic alterations of childhood and adolescence ependymomas and gliomas using the next-generation sequencing strategy” scientific research project, supported by Fundação de Amparo à Pesquisa do Estado de Sao Paulo (The Sao Paulo Research Foundation - FAPESP) and Pediatric Oncology Institute-Grupo de Apoio ao Adolescente e à Criança com Câncer/Federal University of Sao Paulo (IOP-GRAACC/UNIFESP). The authors thank to all the patients and families who contributed to this study.

Author contributions Conceptualization and methodology: SRCT, FTG, IDO; Formal analysis and investigation: DCCC, SRCT, FTG, IDO; Writing—original draft preparation: DCCC; Writing—review and editing: SRCT, FTG, NSS, AMC; Funding acquisition: SRCT; Medical support: NSS, AMC, MTSA, PD, SC; Supervision: SRCT.

Funding This work was supported by grants from Fundação de Amparo à Pesquisa do Estado de Sao Paulo (FAPESP no. 2019/12074-5), Pediatric Oncology Institute-Grupo de Apoio ao Adolescente e à Criança com Câncer/Federal University of Sao Paulo (IOP-GRAACC/UNIFESP), and Coordenação de Aperfeiçoamento de Pessoal de Nível Superior (CAPES).

Data availability The data that support the findings of this study are available from the corresponding author upon reasonable request.

Code availability Not applicable.

Declarations

Conflict of interest The authors declare that they have no conflict of interest.

Ethical approval All procedures performed in studies involving human participants were in accordance with the ethical standards of the Institutional Research Committee (Committee for Ethics in Research—Federal University of Sao Paulo no. 0915/2019). This article does not contain any studies with animals performed by any of the authors.

Informed consent Samples from each primary tumor were collected after informed consent was signed by patients/guardians according to the Institutional Research Committee (Committee for Ethics in Research—Federal University of Sao Paulo no. 0915/2019). The biological material is acquired via a Biobank of the Pediatric Oncology Institute-GRAACC/UNIFESP (National Commission of Ethics in Research—CONEP B-053).

References


Aghajani Y, Levy ML, Malicki DM, Crawford JR (2016) Novel PPP1CB-ALK fusion protein in a high-grade glioma of infancy. *BMJ Case Rep*. <https://doi.org/10.1136/bcr-2016-217189>

- 645 Ahmed AA, Vundamati DS, Farooqi MS, Guest E (2018) Precision
646 medicine in pediatric cancer: current applications and future
647 prospects. *High Throughput* 7(4):39. <https://doi.org/10.3390/h7040039>
- 648 Amatu A, Sartore-Bianchi A, Siena S (2016) NTRK gene fusions as
649 novel targets of cancer therapy across multiple tumour types.
650 *ESMO Open* 1(2):e000023. <https://doi.org/10.1136/esmooopen-2015-000023>
- 651 Amend C, Stadler J, Salamat S, Dedekam E, Waanders A, Wadhvani
652 N (2020) Congenital glioblastoma multiforme: a case report of
653 a rare pediatric brain tumor, molecular analysis, and review of
654 the literature. *Neuro-Oncol* 22(suppl3):iii351. <https://doi.org/10.1093/neuonc/noaa222.324>
- 655 Ballester LY, Meis JM, Lazar AJ et al (2020) Intracranial myxoid
656 mesenchymal tumor with EWSR1-ATF1 fusion. *J Neuropathol*
657 *Exp Neurol* 79(3):347–351. <https://doi.org/10.1093/jnen/nlz140>
- 658 Blattner-Johnson M, Jones DTW, Pfaff E (2021) Precision medicine
659 in pediatric solid cancers. *Semin Cancer Biol.* <https://doi.org/10.1016/j.semcancer.2021.06.008>
- 660 Braunstein S, Raleigh D, Bindra R, Mueller S, Haas-Kogan D (2017)
661 Pediatric high-grade glioma: current molecular landscape and
662 therapeutic approaches. *J Neurooncol* 134(3):541–549. <https://doi.org/10.1007/s11060-017-2393-0>
- 663 Clarke M, Mackay A, Ismer B et al (2020) Infant high-grade gliomas
664 comprise multiple subgroups characterized by novel targetable
665 gene fusions and favorable outcomes. *Cancer Discov* 10(7):942–
666 963. <https://doi.org/10.1158/2159-8290.CD-19-1030>
- 667 De Los SY, Shin D, Malnik S et al (2021) Intracranial myxoid mes-
668 enchymal neoplasms with EWSR1 gene rearrangement: report
669 of 2 midline cases with one demonstrating durable response to
670 MET inhibitor monotherapy. *Neurooncol Adv* 3(1):vdab016.
671 <https://doi.org/10.1093/oaajnl/vdab016>
- 672 Deng H, Zeng J, Zhang T et al (2018) Histone H3.3K27M mobi-
673 lizes multiple cancer/testis (ct) antigens in pediatric glioma.
674 *Mol Cancer Res* 16(4):623–633. <https://doi.org/10.1158/1541-7786.MCR-17-0460>
- 675 Drobyshva A, Klesse LJ, Bowers DC et al (2017) Targeted MAPK
676 pathway inhibitors in patients with disseminated pilocytic astro-
677 cytomas. *J Natl Compr Canc Netw* 15(8):978–982. <https://doi.org/10.6004/jnccn.2017.0139>
- 678 Ebrahimi A, Skardelly M, Schuhmann MU et al (2019) High fre-
679 quency of H3 K27M mutations in adult midline gliomas. *J Cancer Res Clin Oncol* 145(4):839–850. <https://doi.org/10.1007/s00432-018-02836-5>
- 680 Espiritu AI, Terencio BB, Jamora RDG (2020) Congenital glioblas-
681 toma multiforme with long-term childhood survival: a case
682 report and systematic review. *World Neurosurg* 139:90–96.
683 <https://doi.org/10.1016/j.wneu.2020.03.212>
- 684 Fangusaro J (2012) Pediatric high grade glioma: a review and update
685 on tumor clinical characteristics and biology. *Front Oncol*
686 2:105. <https://doi.org/10.3389/fonc.2012.00105>
- 687 Gambella A, Senetta R, Collemi G, Vallero SG, Monticelli M,
688 Cofano F, Zeppa P, Garbossa D, Pellerino A, Rudà R, Soffietti
689 R, Fagioli F, Papotti M, Cassoni P, Bertero L (2020) NTRK
690 fusions in central nervous system tumors: a rare, but worthy
691 target. *Int J Mol Sci* 21(3):753. <https://doi.org/10.3390/ijms21030753>
- 692 Gilani A, Donson A, Davies KD, Whiteway SL, Lake J, DeSisto J,
693 Hoffman L, Foreman NK, Kleinschmidt-DeMasters BK, Green
694 AL (2020) Targetable molecular alterations in congenital glioblastoma. *J Neurooncol* 146(2):247–252. <https://doi.org/10.1007/s11060-019-03377-8>
- 695 Guerreiro Stucklin AS et al (2019) Alterations in ALK/ROS1/NTRK/
696 MET drive a group of infantile hemispheric gliomas. *Nat Commun* 10(1):4343. <https://doi.org/10.1038/s41467-019-12187-5>
- 697 Hargrave D (2009) Paediatric high and low grade glioma: the impact
698 of tumour biology on current and future therapy. *Br J Neurosurg*
699 23(4):351–363. <https://doi.org/10.1080/02688690903158809>
- 700 Hiemzen MC, Ostrow DG, Busse TM et al (2018) OncoKids: a
701 comprehensive next-generation sequencing panel for pediatric
702 malignancies. *J Mol Diagn* 20(6):765–776. <https://doi.org/10.1016/j.jmoldx.2018.06.009>
- 703 Holla VR, Elamin YY, Bailey AM et al (2017) ALK: a tyrosine
704 kinase target for cancer therapy. *Cold Spring Harb Mol Case Stud* 3(1):a001115. <https://doi.org/10.1101/mcs.a001115>
- 705 Hsiao SJ, Zehir A, Sireci AN, Aisner DL (2019) Detection of
706 tumor NTRK gene fusions to identify patients who may benefit
707 from tyrosine kinase (TRK) inhibitor therapy. *J Mol Diagn*
708 21(4):553–571. <https://doi.org/10.1016/j.jmoldx.2019.03.008>
- 709 Huang TY, Piunti A, Lulla RR et al (2017) Detection of Histone H3
710 mutations in cerebrospinal fluid-derived tumor DNA from chil-
711 dren with diffuse midline glioma. *Acta Neuropathol Commun*
712 5(1):28. <https://doi.org/10.1186/s40478-017-0436-6>
- 713 Jiang T, Wang G, Liu Y et al (2021) Development of small-molecule
714 tropomyosin receptor kinase (TRK) inhibitors for NTRK fusion
715 cancers. *Acta Pharm Sin B* 11(2):355–372. <https://doi.org/10.1016/j.apsb.2020.05.004>
- 716 Jones DT, Kocialkowski S, Liu L, Pearson DM, Bäcklund LM,
717 Ichimura K, Collins VP (2008) Tandem duplication producing
718 a novel oncogenic BRAF fusion gene defines the majority of
719 pilocytic astrocytomas. *Cancer Res* 68(21):8673–8677. <https://doi.org/10.1158/0008-5472.CAN-08-2097>
- 720 Jones DT, Gronych J, Lichter P, Witt O, Pfister SM (2012) MAPK
721 pathway activation in pilocytic astrocytoma. *Cell Mol Life Sci*
722 69(11):1799–1811. <https://doi.org/10.1007/s00018-011-0898-9>
- 723 Kao YC, Sung YS, Zhang L et al (2017) EWSR1 fusions with creb
724 family transcription factors define a novel myxoid mesenchymal
725 tumor with predilection for intracranial location. *Am J Surg Pathol* 41(4):482–490. <https://doi.org/10.1097/PAS.0000000000000788>
- 726 Kaul A, Chen YH, Emmett RJ, Dahiya S, Gutmann DH (2012) Pediatric
727 glioma-associated KIAA1549:BRAF expression regulates neuro-
728 glial cell growth in a cell type-specific and mTOR-dependent
729 manner. *Genes Dev* 26(23):2561–2566. <https://doi.org/10.1101/gad.200907.112>
- 730 Korshunov A, Ryzhova M, Hovestadt V et al (2015) Integrated analy-
731 sis of pediatric glioblastoma reveals a subset of biologically
732 favorable tumors with associated molecular prognostic mark-
733 ers. *Acta Neuropathol* 129(5):669–678. <https://doi.org/10.1007/s00401-015-1405-4>
- 734 Lange AM, Lo HW (2018) Inhibiting TRK proteins in clinical cancer
735 therapy. *Cancers (basel)* 10(4):105
- 736 Liu C, Liu Y, Zhao Y et al (2020) Primary intracranial mesenchymal
737 tumor with ewsr1-crem gene fusion: a case report and literature
738 review. *World Neurosurg* 142:318–324. <https://doi.org/10.1016/j.wneu.2020.07.015>
- 739 Lorentzian A, Biegel JA, Ostrow DG et al (2018) Tumor variant identi-
740 fication that accounts for the unique molecular landscape of pedi-
741 atric malignancies. *JNCI Cancer Spectr* 2(4):pky079. <https://doi.org/10.1093/jncics/pky079>
- 742 Louis DN, Perry A, Wesseling P et al (2021) The 2021 WHO classifica-
743 tion of tumors of the central nervous system: a summary. *Neuro Oncol* 23(8):1231–1251. <https://doi.org/10.1093/neuonc/noab106>
- 744 Macy ME, Birks DK, Barton VN, Chan MH, Donson AM, Kleinschmidt-
745 Demasters BK, Bemis LT, Handler MH, Foreman NK (2012) Clinical and molecular characteristics of congenital glioblastoma. *Neuro Oncol* 14(7):931–941. <https://doi.org/10.1093/neuonc/nos125>
- 746 Ng A, Levy ML, Malicki DM, Crawford JR (2019) Unusual high-
747 grade and low-grade glioma in an infant with PPP1CB-ALK gene

- 775 fusion. *BMJ Case Rep* 12(2):e228248. [https://doi.org/10.1136/](https://doi.org/10.1136/bcr-2018-228248)
776 [bcr-2018-228248](https://doi.org/10.1136/bcr-2018-228248)
- 777 Oliveira VF, De Sousa GR, Dos Santos AC et al (2021) Evaluating
778 H3F3A K27M and G34R/V somatic mutations in a cohort of pedi-
779 atric brain tumors of different and rare histologies. *Childs Nerv*
780 *Syst* 37(2):375–382. <https://doi.org/10.1007/s00381-020-04852-8>
- 781 Pollack IF, Agnihotri S, Broniscer A (2019) Childhood brain tumors:
782 current management, biological insights, and future directions. *J*
783 *Neurosurg Pediatr* 23(3):261–273. [https://doi.org/10.3171/2018.](https://doi.org/10.3171/2018.10.PEDS18377)
784 [10.PEDS18377](https://doi.org/10.3171/2018.10.PEDS18377)
- 785 Rolfo C (2020) NTRK gene fusions: a rough diamond ready to spar-
786 kle. *Lancet Oncol* 21(4):472–474. [https://doi.org/10.1016/S1470-](https://doi.org/10.1016/S1470-2045(20)30026-7)
787 [2045\(20\)30026-7](https://doi.org/10.1016/S1470-2045(20)30026-7)
- 788 Schwartzentruber J, Korshunov A, Liu XY et al (2012) Driver muta-
789 tions in histone H3.3 and chromatin remodelling genes in paedia-
790 tric glioblastoma. *Nature* 482(7384):226–231. [https://doi.org/10.](https://doi.org/10.1038/nature10833)
791 [1038/nature10833](https://doi.org/10.1038/nature10833)
- 792 Severino M, Schwartz ES, Thurnher MM, Rydland J, Nikas I,
793 Rossi A (2010) Congenital tumors of the central nervous system.
794 *Neuroradiology* 52(6):531–548. [https://doi.org/10.1007/](https://doi.org/10.1007/s00234-010-0699-0)
795 [s00234-010-0699-0](https://doi.org/10.1007/s00234-010-0699-0)
- 796 Solitare GB, Krigman MR (1964) Congenital intracranial neoplasm.
797 A case report and review of the literature. *J Neuropathol Exp*
798 *Neurol* 23:280–292
- 799 Srinivasa K, Cross KA, Dahiya S (2020) BRAF alteration in central
800 and peripheral nervous system tumors. *Front Oncol* 10:574974.
801 <https://doi.org/10.3389/fonc.2020.574974>
- 802 Sturm D, Witt H, Hovestadt V et al (2012) Hotspot mutations in
803 H3F3A and IDH1 define distinct epigenetic and biological sub-
804 groups of glioblastoma. *Cancer Cell* 22(4):425–437. [https://doi.](https://doi.org/10.1016/j.ccr.2012.08.024)
805 [org/10.1016/j.ccr.2012.08.024](https://doi.org/10.1016/j.ccr.2012.08.024)
- 806 Sturm D, Bender S, Jones DT et al (2014) Paediatric and adult glioblas-
807 toma: multifactorial (epi)genomic culprits emerge. *Nat Rev Cancer*
808 14(2):92–107. <https://doi.org/10.1038/nrc3655>
- Terashima K, Ogiwara H (2021) No shinkei geka. *Neurol Surg* 809
49(3):640–646. <https://doi.org/10.11477/mf.1436204438>
- Venneti S, Garimella MT, Sullivan LM et al (2013) Evaluation of
811 histone 3 lysine 27 trimethylation (H3K27me3) and enhancer of
812 Zest 2 (EZH2) in pediatric glial and glioneuronal tumors shows
813 decreased H3K27me3 in H3F3A K27M mutant glioblastomas.
814 *Brain Pathol* 23(5):558–564. <https://doi.org/10.1111/bpa.12042>
- 815 Wen PY, Packer RJ (2021) The 2021 WHO classification of tumors of
816 the central nervous system: clinical implications. *Neuro Oncol*
817 23(8):1215–1217. <https://doi.org/10.1093/neuonc/noab120>
- 818 Wong A (2017) The emerging role of targeted therapy and immuno-
819 therapy in the management of brain metastases in non-small cell
820 lung cancer. *Front Oncol* 7:33. [https://doi.org/10.3389/fonc.2017.](https://doi.org/10.3389/fonc.2017.00033)
821 [00033](https://doi.org/10.3389/fonc.2017.00033)
- 822 Wu G, Diaz AK, Paugh BS et al (2014) The genomic landscape of
823 diffuse intrinsic pontine glioma and pediatric non-brainstem high-
824 grade glioma. *Nat Genet* 46(5):444–450. [https://doi.org/10.1038/](https://doi.org/10.1038/ng.2938)
825 [ng.2938](https://doi.org/10.1038/ng.2938)
- 826 Yuen BT, Knoepfler PS (2013) Histone H3.3 mutations: a variant path
827 to cancer. *Cancer Cell* 24(5):567–574. [https://doi.org/10.1016/j.](https://doi.org/10.1016/j.ccr.2013.09.015)
828 [ccr.2013.09.015](https://doi.org/10.1016/j.ccr.2013.09.015)
- 829 Zhong Y, Lin F, Xu F, Schubert J, Wu J, Wainwright L, Zhao X, Cao
830 K, Fan Z, Chen J, Lang SS, Kennedy BC, Viaene AN, Santi M,
831 Resnick AC, Storm PB, Li MM (2021) Genomic characterization
832 of a PPP1CB-ALK fusion with fusion gene amplification in a
833 congenital glioblastoma. *Cancer Genet* 252–253:37–42. [https://](https://doi.org/10.1016/j.cancergen.2020.12.005)
834 doi.org/10.1016/j.cancergen.2020.12.005
835

Publisher's Note Springer Nature remains neutral with regard to jurisdictional claims in published maps and institutional affiliations.

Authors and Affiliations

Débora Cabral de Carvalho Corrêa^{1,2} · Francine Tesser-Gamba¹ · Indhira Dias Oliveira¹ · Nasjla Saba da Silva¹ · Andrea Maria Capellano¹ · Maria Teresa de Seixas Alves^{1,3} · Patrícia Alessandra Dastoli^{1,4} · Sergio Cavalheiro^{1,4} · Silvia Regina Caminada de Toledo^{1,2} 

Débora Cabral de Carvalho Corrêa
debora.c.c.correa@gmail.com

Francine Tesser-Gamba
francinegamba@graacc.org.br

Indhira Dias Oliveira
indhirdias@graacc.org.br

Nasjla Saba da Silva
nasjlasaba@bol.com.br

Andrea Maria Capellano
deacapellano@uol.com.br

Maria Teresa de Seixas Alves
mtsaves@unifesp.br

Patrícia Alessandra Dastoli
paty.dastoli@uol.com.br

Sergio Cavalheiro
iscava@uol.com.br

¹ Department of Pediatrics, Pediatric Oncology Institute-GRACACC/UNIFESP, Federal University of Sao Paulo, 743 Botucatu Street, 8th Floor – Genetics Laboratory, Vila Clementino, Sao Paulo, SP 04023-062, Brazil

² Division of Genetics, Department of Morphology and Genetics, Federal University of Sao Paulo, Sao Paulo, SP, Brazil

³ Department of Pathology, Federal University of Sao Paulo, Sao Paulo, SP, Brazil

⁴ Department of Neurology and Neurosurgery, Federal University of Sao Paulo, Sao Paulo, SP, Brazil